Spectral changes and wavelength dependent thermoluminescence of rare earth ions after X-ray irradiation

P.D. Townsend, A.A. Finch, M. Maghrabi, V. Ramachandran, G.V. Vázquez, Y. Wang, D.R. White

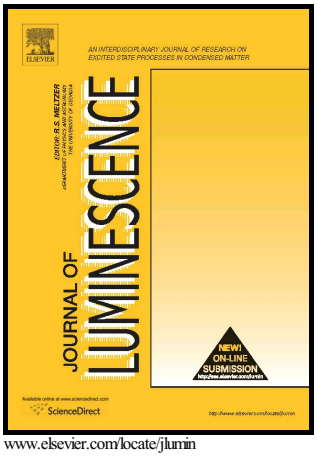

www.elsevier.com/locate/jlumin

PII: S0022-2313(17)30089-3
DOI: http://dx.doi.org/10.1016/j.jlumin.2017.07.041
Reference: LUMIN14917

To appear in: *Journal of Luminescence*

Received date: 20 January 2017
Revised date: 10 June 2017
Accepted date: 21 July 2017

Cite this article as: P.D. Townsend, A.A. Finch, M. Maghrabi, V. Ramachandran, G.V. Vázquez, Y. Wang and D.R. White, Spectral changes and wavelength dependent thermoluminescence of rare earth ions after X-ray irradiation, *Journal of Luminescence* http://dx.doi.org/10.1016/j.jlumin.2017.07.041

Spectral changes and wavelength dependent thermoluminescence of rare earth ions after X-ray irradiation

P.D. Townsend[1], A.A. Finch[2], M. Maghrabi[3], V. Ramachandran[4], G.V. Vázquez[5], Y. Wang[6*], D.R. White[7]

[1] *Physics Building, University of Sussex, Brighton, BN1, 9QH, UK*

[2] *Department of Earth & Environmental Sciences, University of St Andrews, Fife, KY16 9AL, UK*

[3] *Department of Physics, Hashemite University, P.O. Box 150459, Zarqa15 13115, Jordan*

[4] *School of Process & Chemical Engineering, University of Leeds, Leeds, LS2 9JT, UK*

[5] *Centro de Investigaciones en Óptica, León, 37150, Mexico*

[6] *School of Science, China University of Geosciences, Beijing, 100083, China*

[7] *Barnsley Hospital NHS Foundation Trust, Gawber Road, Barnsley S75 2EP, UK*

Abstract

The thermoluminescence spectra of rare earth doped materials after X-ray irradiation typically vary with the glow peak temperature. Additionally, there are many examples where, for the same dopant ion, the expected component emission lines peak, but at different temperatures. This unusual behaviour is discussed in terms of changes in proximity of coupling between trapping and recombination sites. Changes in the energy barriers for recombination influence alternative routes for charge transfer to rare earth sites which can involve different higher energy states of the rare earth dopants. Proposed mechanisms include selective tunnelling, or barrier crossing, in addition to normal charge transfer from remote trapping sites. The model successfully describes numerous examples in terms of the energy scheme for the rare earth ions. Whilst the standard emission lines are recorded in the glow curve spectra they do not always occur at the same temperature, and, even for the same rare earth dopant, they can differ by as much as 30^{o}C. These wavelength dependent variations in peak temperature not only offer information on the proximity of trap and recombination sites, but also introduce issues in conventional activation energy analysis when recording is with polychromatic light. The concepts are relevant for related types of measurement, such as optically stimulated thermoluminescence.

Key words: thermoluminescence; model; wavelength dependent

* Corresponding author, wyfemail@gmail.com

1. Introduction

Luminescence studies offer a highly sensitive probe of defect structures in insulating materials with techniques such as photoluminescence (PL), cathodoluminescence (CL), radioluminescence (RL) and thermoluminescence (TL), etc. Each technique has a vast literature with data from hundreds of materials. It is thus surprising to find a phenomenon that had not previously been noted in the last 60 years of TL data. Nevertheless, the current observations of differences between the TL peak temperatures of a set of emission lines, from the same rare earth dopants, has remained unnoticed. This article summarises these unfamiliar features that have been observed from several types of material with the same high sensitivity spectrally resolved TL equipment.

Thermoluminescence is of particular importance because of its applications in radiation dosimetry, as well as the ability to thermally separate different features from trapping and luminescence sites [e.g. 1-3]. Polychromatic recording is invariably used for dosimetry, but for more fundamental analyses the TL heating data require detailed spectral recording. Broad band luminescence spectra are common features linked to intrinsic defect sites; by contrast, signals from rare earth dopants are characterised by narrower bands, or line spectra. In each case, there can be both changes in the overall emission pattern with temperature and movements of the peak wavelengths. Major spectral changes are normally considered to be evidence of different defect sites. In continuously excited signals (PL, CL or RL) steady spectral movements as a function of temperature can indicate that the relevant defect sites are basically unchanged. By contrast TL signals occur over limited temperature ranges resulting from charge transfer between trapping and recombination sites. Here the temperature monitors the transfer barrier, even if the emission site is common to many TL peaks. The TL spectra from rare earth sites can vary significantly in terms of the number of lines, and their relative intensities. Such differences are unlikely if there is separation of the traps and the

rare earth (RE) recombination sites, thus close links between traps and the rare earth sites must be considered.

2. Evolution of Thermoluminescence models

Thermoluminescence (TL) is a simple process in which exposure to ionizing radiation, or UV light, can produce free electrons and/or holes. These become trapped at imperfections. Subsequent heating releases the charges and, during their recombination and return to a ground state, the energy release is in the form of light. This is a potential dosimeter for ionizing and UV radiation, as in favourable conditions the trapping sites are stable at ambient temperature, and eventually the read-out stage offers an integrated signal proportional to the radiation exposure. A high percentage of insulating materials display TL; the personnel dosimetry market is large, and so there have been hundreds of publications proposing new, or better, dosimeters. In the initial idealised models, Fig. 1, the trapping and recombination sites were assumed to be separate and it was then simple to model the processes in terms of a trap depth (E) and an attempt to escape frequency (ν). For applications, the progress has been with a mixture of understanding the complex properties of imperfections and intelligent empirical experimentation. The requirements are a material that is stable during storage, produces a high light output for a small radiation exposure, and emits strongly in the frequency range where photomultiplier tubes are efficient. High heating rates improve dosimetry analysis by reducing background noise, although they compromise accurate temperature measurements.

Even by the 1960s it was apparent that for successful dosimeters, such as TLD100, the simplistic model was inappropriate. This material is doped LiF, which is a favourable equivalent for radiation absorption in tissue. The TLD 100 includes Mg^{2+} ions located on Li^{+} lattice sites, with size and charge compensation of the Mg^{2+} via an adjacent Li vacancy. For thermal stability of storage, the site is heat treated to form a ring of three units. A closely linked trapping site means the trap to luminescence pathway is very efficient, and this is

provided with Ti^{4+} ions directly associated with the ring of Mg-$Li_{vacancy}$ units. Further charge compensation (for Ti^{4+} ions on Li^{+} sites) is needed in the form of O^{2-} ions on fluorine sites. In reality, this package is totally different from the idealised model of well separated independent trapping and luminescent sites. Many other dosimeter models have been cited [e.g. 1- 3].

Advances in understanding impurity sites show that charge compensation, and minimisation of lattice strain energy, invariably cause close association of impurities and compensators, and, in extreme cases, precipitation of dopants into new phases. Hence, there can be a multiplicity of very similar traps and luminescence sites. Many rare earth (RE) examples are documented via techniques such as site selective spectroscopy [4, 5] in which scanning with high resolution excitation spectra reveal equally detailed changes in the emission from nominally the same type of rare earth site. Luminescence does not provide lattice structure details, but in paramagnetic resonance studies of RE ions, such as ENDOR (electron nuclear double resonance) [6], the local distortions of the lattice are observable over many neighbouring atoms. Even more distant trap/recombination site interactions have been monitored. For example, at low temperature, a shifting pattern of exciton emission data from GaP [7] was modelled to confirm that pair-related exciton line spectra from electron/hole binding were measurable up to separations of some 50 neighbouring ionic shells.

The long-range interactions between rare earth dopants and structural defects are also evident in technological applications, such as rare earth laser systems, where the impurity clustering as a function of dopant concentration, and interactions with defects (from surfaces, dislocations, and intrinsic defects) all change the luminescence properties of relative intensity of emission lines, excited state lifetimes and laser performance [8].

Overall, the defect literature indicates considerable complexity, and distortions in the imperfections and these are apparent in a sensitive technique such as TL. In reality it also

implies non-unique activation energies if there are a range of similar sites with small changes in local distortions. TL kinetics of a band of activation energies have similarly been discussed in mineral systems where there are structural variations between different ordered and disordered phases [9]. Such subtle site variations are obscured in polychromatic TL recording, and irrelevant for dosimetry applications. However, addition of good resolution spectral detail offers many insights into the many defect interactions, especially from rare earth sites. For precise temperature analysis both low heating rates, in order to have accurate temperature control [10], and high sensitivity wavelength multiplexed spectral acquisition are essential. This precision can separate the many defect processes which are present. Successes with the present system are many (e.g. as reviewed in reference 11). For example, in numerous host lattices the rare earth dopants show displacement of the TL peak temperature in a systematic pattern depending on the size of the impurity ion relative to the host site. Particularly clear examples were reported for RE-doped LaF_3 and $Bi_4Ge_3O_{12}$ in which the changes in TL peak temperature are a smooth function of the ionic size. The LaF_3 data also indicate that the RE ions are clustered into groups of at least three dopants (i.e. a similar pattern to that of TLD 100). Dopant clustering and association with intrinsic defects was exemplified by changes in the spectra and peak temperatures of Nd-doped CaF_2 where changing Nd concentrations and/or thermal treatments, totally modify the TL spectral data and generate different balances between the Nd line spectra, as well as changes in band width, plus intrinsic broad band emission. Extreme examples of clustering revealed by TL data include impurity phase precipitation of rare earth dopants in zircon [12] and impurity nanoparticle precipitates [13].

Overall the improvements in understanding the complexity of defect structures, and their influence on TL has moved a long way from the simplistic original thoughts on isolated unique-valued parameters of TL, as envisioned in the historic models. These did not consider

the present thoughts on changing rare earth emission spectra with glow peak temperature, nor the possibility that, from the same rare earth dopant, the emission wavelengths could differ in their TL temperature. However, in hindsight, one can sense these features in earlier publications. Defect models now require the realisation that many of the sites are complexes of dopants and impurity sites, and indeed the traps and recombination sites may be intimately linked.

3. Experimental background

The thermoluminescence data discussed here were collected with a sensitive wavelength multiplexed spectrometer system [14]. Collection spans temperature ranges from 20 to 673 K. (Note, however, that dosimetry data are conventionally discussed in ^{o}C). Since the data are either collected with a cryostat in a low temperature range from 20 to 300K, or with a heater system above room temperature, the discussion refers to these different systems as low or high temperature TL. In order to have good thermal contact in the low temperature range, where thermal conductivity of insulators is poor, the cryostat is typically heated at 6 degrees per minute, but above room temperature 15 degrees per minute maintains thermal control. By contrast, the TL dosimetry recording systems may operate at a heating rate of 300 degrees per minute as only the integrated signal is important.

Excitation of thermoluminescence was with X-ray irradiation either at 20K (for the "low" temperature data, or at room temperature for the "high" temperature TL measurements. The X-ray energies used were variously 15, 20 or 25 keV. Radiation doses were typically 5 Gy.

High spectral sensitivity is achieved with f/2.2 optics, and two diffraction grating spectrometers using photon imaging tube detectors (from Photek Ltd, UK). The use of two gratings allows grating and detector optimisation for each of the UV/blue and green/red spectral regions. It also avoids signals produced by second-order diffraction, and high grating efficiency is maintained over the entire range of each spectral range. The Photek detectors

have peak quantum efficiencies of ~ 50%. In addition to TL, the system has facilities for RL, CL and PL.

Samples described here range from rare earth dosimetry powder of rare earth doped magnesium orthosilicate from The China University of Geosciences, to single crystals of Nd:YAG (Roditi corporation) and alkaline earth fluorides (Harshaw Chemical company and the University of Kent).

4 Multiline rare earth spectra recorded during thermoluminescence.

As mentioned, an oversight of previous analyses was to not recognise that for a multiline emission spectrum from rare earth ions the glow peak temperatures are not identical at each wavelength. The changes are not random but, as shown below, are linked to the higher-energy states of the ions that define the emission wavelength. Two clear examples of this effect are apparent in the spectra of TL from terbium or europium doped magnesium orthosilicate dosimetry powder [15]. Conceptually, these are not ideal examples as the dosimetry powders are sensitive to dopant concentration and their thermal processing. However, there are many other examples of RE ions in crystalline hosts that display identical behaviour, and some will be mentioned.

Figure 2 presents low temperature TL spectra from Tb-doped Mg_2SiO_4 in the form of isometric (Fig. 2(a)) and contour (Fig. 2(b)) displays. This variant is for 5wt% Tb after sintering for 6 hours at 1500 ^{o}C. The signals are dominated by Tb emission, and at low temperature in this material no signals are present from the host lattice. By contrast, host effects are often seen in data above room temperature. Detailed analysis, however, shows that the 7 strong Tb emission lines do not peak in their TL patterns at identical temperatures. Values are listed in Table I.

The same behaviour pattern is noted during heating whilst recording the radioluminescence (RL), as included on Fig. 2(c). Heating to stimulate RL at just 6 K/minute

means that not only does one generate RL from the system, but there is an additional component from the ionisation that adds a TL component to the signal. Whilst this is normally an unwanted feature it has the benefit that for all lines the signals are strong and, as in this case, temperature differences between responses of different Tb transitions are evident. Note that the continuous stimulation with RL prolongs the TL component, and so the peak temperature is normally slightly raised.

TABLE I. TL Peak temperatures of the Tb dopant at different wavelength
(Here the data are for a magnesium orthosilicate dosimeter with 5wt% Tb sintered for 6 hours at 1500 ^{o}C)

Wavelength (nm)		**377**	**417**	**440**	**488**	**550**	**585**	**622**
TL	Peak, K	213	213	213	212	210	210	216
RL	Peak, K	220	220	220	217	216	216	223

Wavelength (nm)		**383**	**420**	**444**	**488**	**551**	**595**	**623**
TL	Peak, ^{o}C	36	36	36	36	36	36	36
TL	Peak, ^{o}C	130	133	133	133	133	133	131
TL	Peak, ^{o}C	294	294	294	294	294	294	294

Figure 3 presents the TL from the same material in measurements above room temperature. In this higher temperature data, there are no differences in peak temperature between different Tb emission lines for this variant of the dosimeter powder. The emission pattern is similar, but not identical, with that at low temperature.

For this type of Tb doped dosimeter material (5wt% Tb and sintered for 6 hours at 1500 ^{o}C) the low temperature data show the longer wavelength emissions peak at a lower temperature than those at shorter wavelengths (except for the 622nm emission). The differences are small, but readily resolved at this heating rate of 6 K/min. By contrast, a more sensitive, and differently processed variant of the Tb doped Mg_2SiO_4 dosimeter powder (1wt % Tb, sintered at 1650 ^{o}C) has shown high temperature differences in peak temperature with wavelength. In that example, the data were collected at the very high heating rate of 300

K/min as used in radiation dosimetry. Values are included on Table II and they also show a definite wavelength dependence on peak temperature.

TABLE II. High temperature glow peaks for Mg_2SiO_4:Tb taken under dosimetry conditions. (Data for magnesium orthosilicate dosimeter powder with 1wt% Tb sintered for 6 hours at 1650 ^oC)

Wavelength (nm)		**383**	**420**	**444**	**484**	**551**	**595**	**623**
TL	Peak, ℃	313	313	313	313	317	317	317
TL	Peak, ℃	377	377	377	377	387	387	383

Tb has possible transitions at both 488 and 484 nm from different upper states, but for the broadened lines of TL, and the spectral resolution used in the current experiment, one does not clearly separate these lines. Nevertheless, the grouping of the lines in terms of peak temperature suggests that they are both present. The transitions are indicated on Fig. 4.

5. A model for wavelength dependent TL variations

The transition wavelengths have been indicated in Fig. 4 with the patterns from Dieke [16] who lists RE transitions in a LaF_3 host. The Tb signals match those labelled as producing luminescence. Historically the energies were in wavenumbers, as used in this figure, together with electron volt energy units. In the unresolved spectral region near 484 to 488 nm the 488 nm (from the upper state of $^5D_4$) is dominant for the low temperature data, whereas the 484 nm transition from $^5D_3$ is indicated in the dosimetry data of Table II. The energy scheme therefore consistently links the difference in TL peak temperature (for both tables) to the upper states of the Tb ion. In the low temperature data, the lines at 377, 418 and 484 nm all appear at slightly higher temperatures than those at 488, 554, 587 and 624 nm in TL, and are matched by a parallel difference in the RL heating results. In dosimetry data above room temperature the only difference appears to be that the 484 nm emission is clearly present in the higher state group. Note there is an anomaly that the weak 624 nm emission fits the same energy scheme, but in both the TL and RL values it is some 6 degrees higher than the others originating at the $^5D_4$ level.

The correlation between peak temperature and upper state is feasible since the orbital extent of the higher states is greater and this will allow them to couple to a larger volume of the surrounding neighbours than the lower level states. Hence upper and lower states will differ in their ability to gain electrons from nearby traps, because the conditions of tunnelling and barrier crossing will differ for each excited state.

Since close proximity of traps and recombination sites can be maintained at low temperature, wavelength dependent responses influenced by orbital extent will be more pronounced at low temperatures. Well separated trap and recombination sites will be less sensitive to orbital extent. Three possible situations are shown in Fig.5 that would result in wavelength differences in peak temperature.

At the lowest temperatures, extremely close coupling will initially allow electron transfer by tunnelling, and then subsequently by barrier crossing. Hence electrons may first feed directly to the set of L states. This would generate a TL peak at long wavelengths which precedes any short-wavelength signals (from H levels). It is the mechanism shown in Fig. 5 (i). After depletion of immediate neighbour traps, higher temperatures will allow linkage to more distant neighbours (case ii). Here preferential transfer to the L states is inhibited but transfer to the H levels may still commence by tunnelling. With further heating the higher temperatures will allow barrier crossing that will feed both higher-level H states and also the lower-level L rare earth states. The effect is that for this intermediate situation the glow peaks of higher states will occur first. With continued heating to higher temperatures, electrons will cross the barrier and feed all H levels, so there is a changing competition between the states, and relatively the TL intensity from high states will decrease. Finally, for distant sites only long-range charge transport is possible and in this case the competition between transitions from H and L states will be insensitive to temperature (i.e. effectively the classical model of Fig. 1).

These three options successfully describe all the data seen here for both types of Tb-doped dosimeter powders. In the case of the Tb doped material reported in Table I the observations suggest that the type (i) tunnelling contribution will initially drive long wavelength emission, giving the peak at 210 K. As the temperature is increased, the balance moves to favour higher-level states, and then this signal peaks at 213 K (i.e. type ii). Above room temperature for this material (at low heating rates) the dominant pathway is from far more distant trapping sites (type iii). Therefore, at the highest temperatures there is minimal difference between the population of the L and H starting levels (i.e. all signals will display the same glow peak temperature).

By contrast for the data of Table II the temperature range in the dosimetry measurements is high (i.e. well above room temperature) so very close trap and RE sites will already have been depleted. In this situation, only mid to long range types of defect sites will be stable. The spectral split between peaks at 377 and 387 ^{o}C will then fit the mid-range pattern of Fig. 5 (ii).

6. Examples of wavelength TL differences from single crystal samples

The dosimeter examples involved extreme heating treatments in their optimisation which generate and retain many intrinsic defects, and are taken for powder grain material where any surface effects may be significant. Many similar features have been noted for RE ions in single crystal hosts and one such, which also reveals the role of thermally generated defects, is for 0.1% Er doped CaF_2 crystals. Above room temperature there are several emission lines, but the signals are primarily in the green from wavelengths of 525 and 537 nm. As received, these have glow peaks at 155 and 150 ^{o}C. After a heat treatment to 500 ^{o}C the TL shifts in temperature depending on the rate of cooling (i.e. this causes differences in the association and retention of intrinsic defects). Slow cooling moves the peaks to 228 and 222 ^{o}C, whereas rapid cooling shifts them to 197 and 202 ^{o}C. The changes are displayed on

the contour plots of figure 6. In each case, there is a temperature difference in the TL of the two lines of ~6 degrees. Overall the data fit the tunnelling variant of Fig. 5 (ii) independent of peak temperatures increase by ~20% from ~425 to 498 K. (The 20% difference in peak temperature implies a 20% change in binding energy resulting from alternative associations with defects in the lattice).

Further examples have been noted in materials as diverse as Nd:YAG and Eu-doped magnesium orthosilicate powder. In the TL of Nd:YAG, after electron irradiation, there are many strong emission lines and their relative intensities change when comparing Nd:YAG single crystal and powder material. There are three main low-temperature peak regions near 75, 130 and 160 to 200 K for powder and a single broader set of peaks with a main maximum near 120 K. Peaks at wavelengths of 400, 553, 625 and 808 nm all follow nominally the same pattern but in both powder and single crystals the 710 nm line emission is displaced to higher temperatures. For powder, the displacements of the lower features are by almost 3 degrees, whereas in the single crystal the peak near 120 K is displaced to higher temperatures for the 710 nm emission by ~ 15 K. This behaviour is consistent with the model of Fig. 5 (ii). In terms of the upper energy levels the 710 nm emission originates from a lower state ($^2H_{11/2}$) than any of the other lines, and thus is at too low an energy level to be populated by tunnelling, whereas this is feasible for the other emission lines (i.e. it is totally consistent with the proposed model).

To underline that the role of defects adds complexity to the TL, as well as shifting the TL peak temperatures, Table III summarises the differences between the strong low temperature TL feature from a single Nd:YAG crystal before and after grinding it into a powder form. There are more TL peaks from the powder material but they are not as cleanly separated as the example cited in the table. However, the overall effect is to demonstrate that defects alter the luminescence properties, whether induced by thermal treatments, or by

mechanical damage. Further, the anomalous behaviour of the 710 nm emission (relative to the other emission lines) is apparent to a lesser extent in the highly defective material.

Table III Changes in the anomaly of the main low temperature TL peak from the 710 nm emission from Nd:YAG in a crystal and a powdered material.

Wavelength (nm)	**Crystal TL K**	**Powder TL K**
400, 553, 625, 808	~116	~133.5
710	~129	~136.2
Difference in K	~13	~2.7

The Eu example of a magnesium orthosilicate powder, Fig. 7 [15] has all the features of types (i), (ii) and (iii) as it successively adds in higher starting states with higher glow peaks temperatures. At low temperature, long wavelength emission occurs, but at high temperature many more lines are activated. Analysis in terms of conventional TL is difficult as the peak separations may be interpreted in terms of distinctly different trapping sites, rather than different means of communication from a trapping site to the RE recombination centre. Values of the peak temperatures and wavelengths are included in Table IV.

TABLE IV Eu peak temperatures for low- and high-temperature TL signals
(Data are for a magnesium orthosilicate dosimeter with 5wt% Eu sintered for 6 hours at 1500 ^{o}C)

Wavelength (nm)	487	545	598	614	654	699	721
TL Peak (K)	-	-	85	85	-	-	-
TL Peak (K)	-	-	105	105	-	-	-
TL Peak (K)	-	-	227	241	-	217	217
TL Peak (K)			-	277	-	-	-
Estimates	~310	~300					
Wavelength(nm)			594	611	654	690	707
TL Peak (^{o}C)			111	111	111	111	111
TL Peak (^{o}C)			211	211	254	255	255

As for Tb, the temperature dependence can be matched to increasingly higher excited states of the various luminescence lines of the Eu ion, as sketched on Fig. 8.

As a final example, Fig. 9 displays TL from a SrF_2 crystal, lightly doped with 0.01% of Er. The isometric spectral plots reveal many emission lines from the Er dopant. At low temperature, the Er lines are resolved and are the only signals. There is no emission below 400 nm. By contrast, above room temperature there are very many peaks and emission features, including a broad band (near 300 nm) which might arise from intrinsic defects of the crystal. The contour map indicates that the various Er emission lines peak at many different temperatures. Near 60 ^{o}C three lines are apparent and their temperature values rise slightly for shorter wavelengths; by 120 ^{o}C the pattern is repeated, but only 2 lines are clearly present. All these initial temperature peaks are consistent with very closely linked trap with coupling by tunnelling as modelled in Fig. 5 (i).

The various emission lines (and band) in the range from 190 to 220 ^{o}C commence with a small temperature separation of the 525 and 545 nm lines, followed by the 670, 600-650, 487, 442 and 406 nm lines, and finally the broad band near 300 nm. Thus, the one nominal glow peak comprises at least 8 different component features that are wavelength sensitive. This clarity of separation of peak temperature with increasingly higher starting levels of the Er occurs because all the transitions are from higher levels down to a single ground state (i.e. in contrast with say the Tb and Eu data discussed earlier) [15]. From the modelling of Fig. 4 the entire pattern for Er in this host is from successively more distant (but linked) trapping sites by a mixture of tunnelling followed by barrier crossing.

7. Discussion and implications

The examples selected here consistently demonstrate that the TL peak temperatures of rare earth line emissions are not identical. The various glow peaks frequently include different numbers of the set of possible rare earth lines and the relative line intensities are not constant [e.g. 11 and references therein]. Data from examples with different RE ions in a variety of host lattices, consistently record changes as a function of dopant concentration, both from variations in the glow peak temperatures, and in the relative intensities of the

emission lines. All such features are in accord with models for RE emission sites that are closely associated with intrinsic defects, together with strong linkages to other RE dopants. The example of RE dopants in LaF_3 suggested that the luminescence sites can contain 3 or more dopants, even though there is no requirement for charge compensators. Similarly, the fact that the emission spectra can differ with glow peak temperature implies that there is normally a direct linkage between most trapping and RE emission sites. For isolated traps and RE emission sites one assumes the spectra would be independent of the defect if charge was being transferred via the conduction band. In which case there is no selectivity on the population of the higher energy states, so all wavelengths will then have TL signals at the same temperature, and all will exist at each TL peak.

As noted for the example of exciton emission of GaP [7] extremely long-range interactions exist. Indeed, interactions with surfaces, dislocations and intrinsic defects means that even in very high-grade material (such as rare earth doped laser crystals) the excited state lifetimes and luminescence emission are dominated by defect interactions [8].

All such evidence supports the proposed model of charge capture from closely associated traps. Here the alternatives are phrased in terms of transfer of charge via either tunnelling or barrier crossing routes. But one cannot exclude the fact that in the many structural variants of the trap and RE site combinations there may be some situations of a low barrier which is indistinguishable in TL from a tunnelling process. Steady-state luminescence decay over a range of temperature may offer a distinction as the kinetics of tunnelling can be athermal [1, 17].

The data support the concept that there is frequently a range of close associations of dopants, defects, charge compensators and lattice distortions to minimize the free energy and/or maintain charge equilibrium. The direct links between trap and recombination sites are

desirable as they offer a high luminescence efficiency. Such close proximity favors charge transfer by tunneling, and/or by crossing the intervening energy barrier.

Whilst these data are informative in terms of modelling the various sites and their separation, it implies there will be significant errors in the simplistic determinations of activation energies that are derived from polychromatic signal recording. The rather extreme example with Er shown in Fig.9 indicates that the peak values spread over ~30 degrees. Conventional TL activation energy analysis with polychromatic signals would therefore be seriously compromised (fortunately it does not change the usefulness of the dosimetry).

The present model also has implications for optically stimulated TL and related techniques, such as infra-red stimulation of luminescence, in dosimetry studies [e.g. 18 - 22] where the temperature dependence of tunneling is often considered. However, such data often involve broad emission bands and are therefore more difficult to interpret compared with the current examples of wavelength dependence of the TL from rare earth sites.

A final comment is that, even for luminescence studies for dosimetry (and other applications), it is evident one requires data, with spectral details, over a wide temperature range. The present data are the product of a highly sensitive, wavelength multiplexed spectrometer, with a wide temperature range, and alternative excitation methods. More general construction and use of such systems therefore seems to be a necessary, and informative, addition for many luminescence and surface studies.

Acknowledgement

One of the authors, Y. Wang would like to thank the support of the Fundamental Research Funds for the Central Universities of China, the National Natural Science Foundation of China (No.51472224, No.11205134), and Beijing Higher Education Young Elite Teacher Project (YETP0640). We also thank Professor SWS McKeever for critical and perceptive supportive comments on this paper.

References

[1] S.W.S. McKeever, Thermoluminescence of solids, Cambridge University Press, Cambridge, 1985.

[2] S.W.S. McKeever, M. Moscovitch, and P.D. Townsend, Thermoluminescence dosimetry materials: Properties and uses, Nuclear Technology Publishing, Ashford, 1995.

[3] R.Chen and S.W.S. McKeever, Theory of thermoluminescence and related phenomena, World Scientific, Singapore, 1997.

[4] G. Lifante, F. Cussó, F. Jaque, J.A. Sanz-García, A .Monteil, B. Varrel, Site-selective spectroscopy of Nd^{3+} in $LiNbO_3$: Nd and $LiNbO_3$: Nd, Mg crystals, Chemical physics letters 176 (1991) 482-488.

[5] J. Garcia Sole, A. Monteil, G. Boulon, E. Camarillo, J. Tocho, I.Vergara, F. Jaque, Site selective spectroscopy of Nd^{3+} and Cr^{3+} sites in $LiNbO_3$ crystals codoped with Mg^{2+} ions, Journal de Physique IV Colloque, 01 (C7) (1991) 403-406.

[6] A.A. Kaplyanskii, R.M. McFarlane, Spectroscopy of Crystals Containing Rare Earth Ions, Amsterdam, 2012.

[7] W. Hayes and A.M. Stoneham, Defects and defect processing in nonmetallic solids, Wiley, New York, 1985.

[8] Fuxi Gan, Laser Materials World Scientific, Singapore, 1995. ISBN 981-02-1580-0

[9] L. Sanchez-Munoz, J. Garcia-Guinea, P.D. Townsend, T. Juwono and A. Cremades, Gaussian thermoluminescence in long-range disordered K-feldspar, American Mineralogist 101 (2016) 2118-2122.

[10] A. Ege, Y. Wang and P.D. Townsend, Systematic errors in thermoluminescence, Nucl. Insts. Methods A 576 (2007) 411-416.

[11] P.D. Townsend, B. Yang and Y. Wang, Luminescence detection of phase transitions, local environment and nanoparticle inclusions, Contemp. Phys. 49 (2008) 255-280.

[12] T. Karali, N. Can, P.D. Townsend, A.P. Rowlands and J. Hanchar, Radioluminescence and thermoluminescence of rare earth element and phosphorus-doped zircon, American Mineralogist 85 (2000) 668-681.

[13] P.D. Townsend, A.A. Finch, M. Maghrabi, V. Ramachandran, G.V. Vazquez, Y. Wang, and D R. White, Luminescence detection of nanoparticle inclusions from their phase transitions, J. Applied Physics, 121 (2017) 145101.

[14] B.J. Luff and P.D. Townsend, High sensitivity thermoluminescence spectrometer, Sci. Technol. 4 (1993) 65-71.

[15] Y. Zhao, Y. Zhou, Y. Jiang, W. Zhou, A.A. Finch, P.D. Townsend and Y. Wang, Ion size effects on thermoluminescence of Terbium and Europium doped Magnesium Orthosilicate, J. Mater. Res. 30 (2015) 3443-3452

[16] G.H. Dieke, Spectra and energy levels of rare earth ions in crystals, Wiley, New York, 1968, p.142

[17] R. Visocekas, Tunnelling in Afterglow: its Coexistence and Interweaving with thermally Stimulated Luminescence, Radiat Prot Dosimetry 100 (2002) 45-53.

[18] F.D. Walker. L.E. Colyott. N. Agersnap Larsen, S.W.S. McKeever, The wavelength dependence of light-induced fading of thermoluminescence from α-Al_2O_3:C, Radiation Measurements, 26 (1996) 711-718.

[19] M. Jain, C. Ankjærgaard,. Towards a non-fading signal in feldspar: Insight into charge transport and tunnelling from time-resolved optically stimulated luminescence Radiat. Meas (2011). 46(3), 292-309.

[20] M. Jain, B. Guralnik, M.T. Andersen, Stimulated luminescence emission from localized recombination in randomly distributed defects, J. Phys.-Conden. Matt., 24 (2012) 385402.

[21] G. Kitis, V. Pagonis, Analytical solutions for stimulated luminescence emission from tunneling recombination in random distributions of defects, J. Lumin.137 (2013) 109-115.

[22] G. Kitis, G.S. Polymeris, I.K. Sfampa, M. Prokic, N. Meric, V. Pagonis, Prompt isothermal decay of thermoluminescence in MgB_4O_7:Dy, Na and LiB_4O_7:Cu dosimeters, Radiat. Meas. 84 (2016) 15-25.

Figure captions

Fig. 1. An early simplistic model for thermoluminescence with totally independent trapping and recombination sites and charge transport via the conduction band.

Fig. 2. An isometric view of the TL emission spectra at low temperature TL for a Tb doped Mg_2SiO_4 dosimeter powder (5wt% Tb sintered for 6 hours at 1500 ^oC). The contour view is restricted to the main features. The third image is for the RL isometric plot recorded during heating.

Fig. 3. Spectrally resolved TL isometric for Tb doped Mg_2SiO_4 dosimeter powder (5wt% Tb sintered for 6 hours at 1500 ^oC) above room temperature. Note the high temperature signal beyond 650^oC is merely black body emission.

Fig. 4. The energy level scheme for Tb transitions from Dieke [16], transition wavelengths are in nm.

Fig. 5. Luminescence transitions originate from the H and L energy levels of the RE ion down to the ground states, G. The three sketches show (i) a very close coupling between the trapping site and the rare earth ion; (ii) a more distant linkage and (iii) a remotely separated trap and rare earth. During heating the options first favour tunnelling (dotted lines) and then barrier crossing, so different states will be involved as a function of temperature, even for the same trapping site. For (iii) no tunnelling is feasible so charge transfer is via the conduction band.

Fig. 6. Varations in the high temperature TL of the same 0.1% Er doped CaF_2 single crystal as the result of heat treatments. The contour maps are for (a) the original sample; (b) after annealing at 500 ^oC and slow cooling, whereas in (c) there had been rapid cooling. Note the temperatures of the TL emission are displaced by the heat treatments. Further, the emission lines at 525 and 537 nm differ in peak temperature by ~6 degrees in each case.

Fig. 7. The figures contrast the spectral changes in the TL of Eu doped Mg_2SiO_4 dosimeter material (1wt% Tb sintered for 6 hours at 1650 ^oC) as a function of temperature. The data are obtained in two steps using a low (20K) and high (room) temperature irradiations. Note the spectral range is limited above room temperature as there were no signals below ~550nm.

Fig. 8. The assignment of the observed Eu transitions using the energy levels shown by Dieke [16], wavelengths are in nm.

Fig. 9. The TL examples display emission spectra from a crystal of Er doped SrF_2. At low temperature, there are strong signals confined to a limited spectral range. Above room temperature the lines are broader and span more of the spectrum. The emission lines not only change in terms of relative intensity, but their TL peaks occur at distinctly different temperatures.

Fig 1

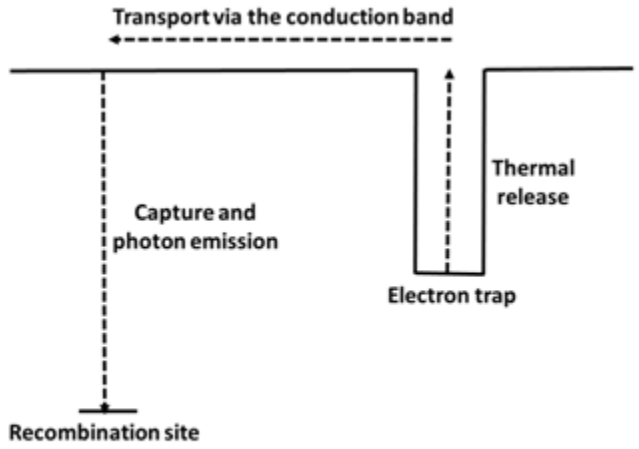

Fig. 1.

fig 2

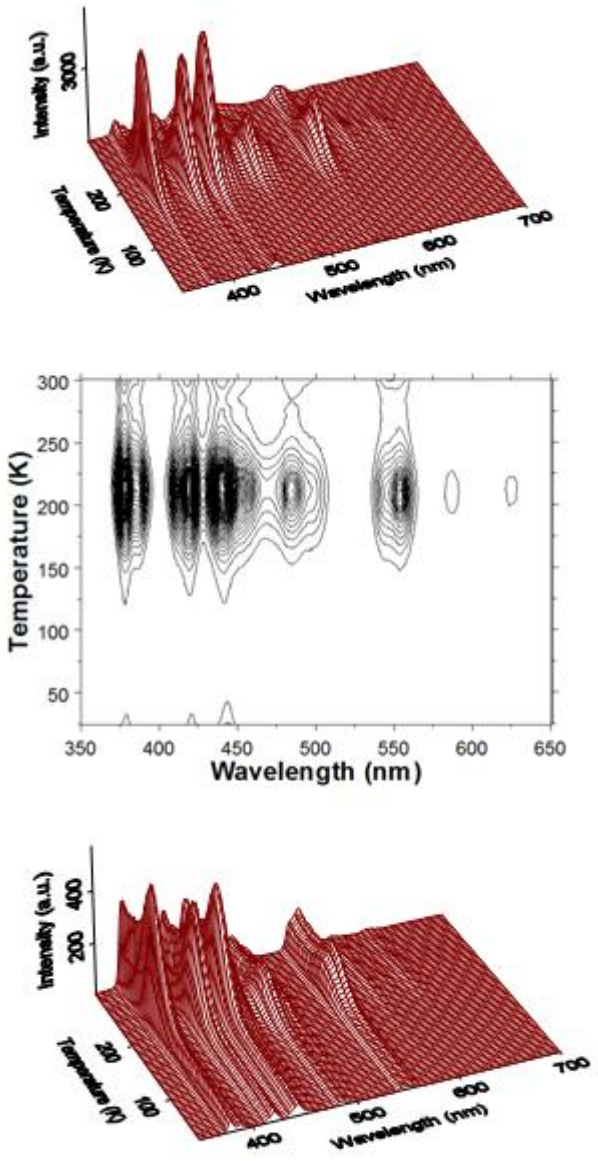

Fig. 2.

fig 3

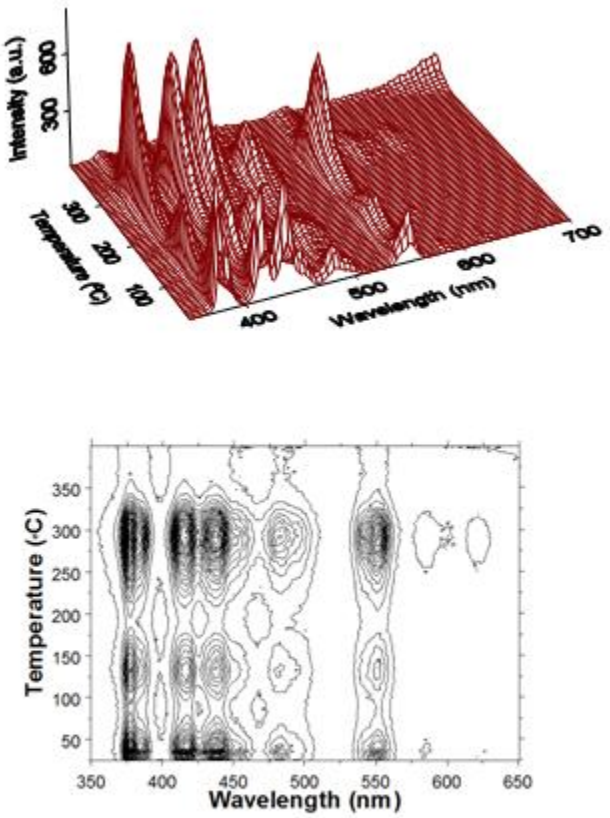

Fig. 3.

fig 4

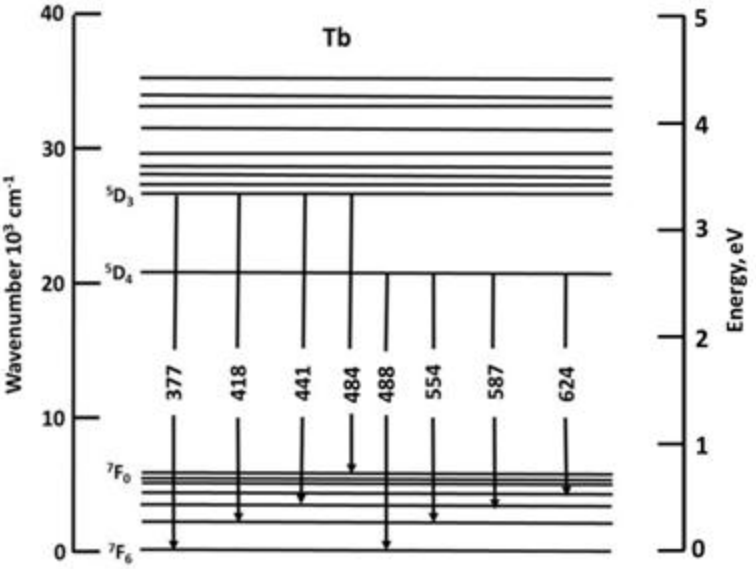

Fig. 4.

fig 5

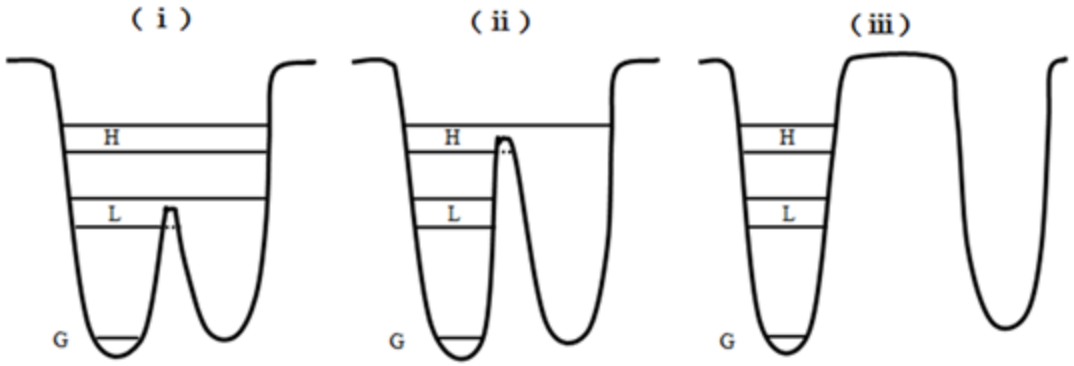

Fig. 5.

fig 6

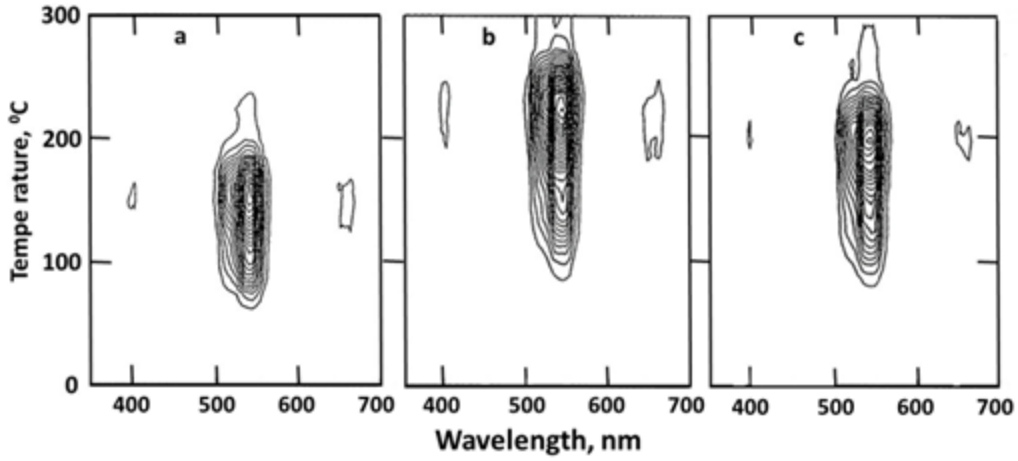

Fig. 6.

fig 7

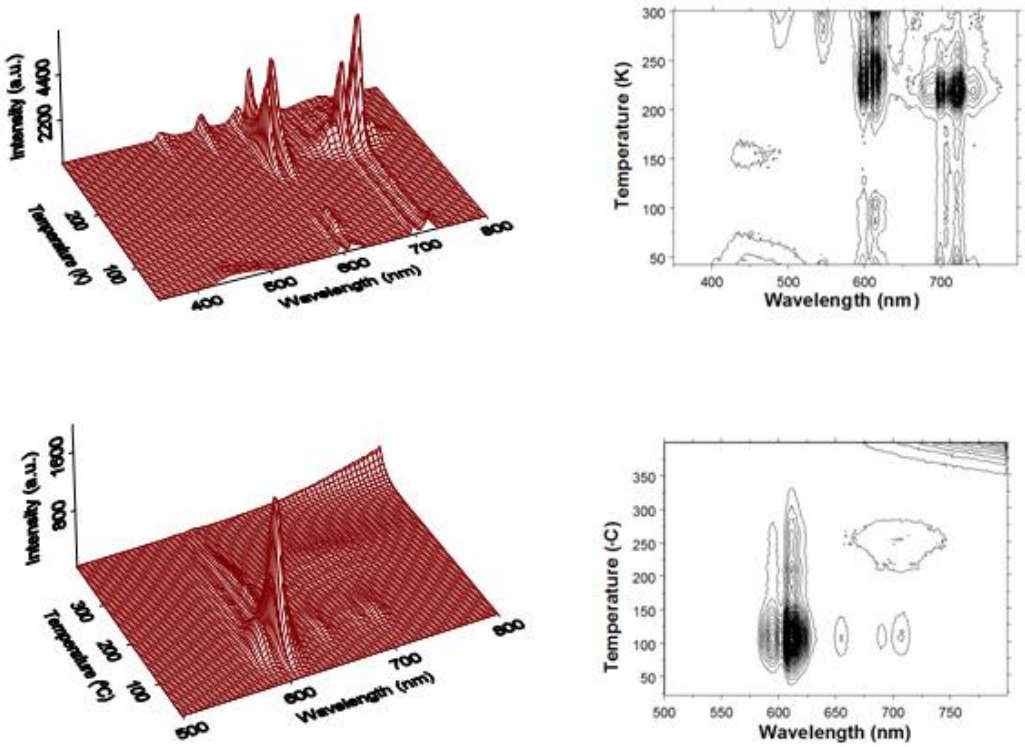

Fig. 7.

fig 8

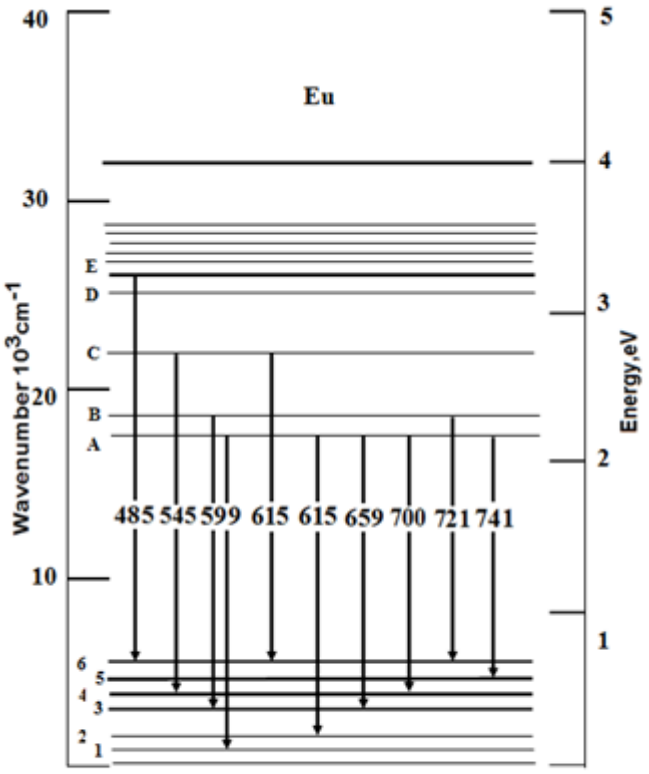

Fig. 8.

fig 9

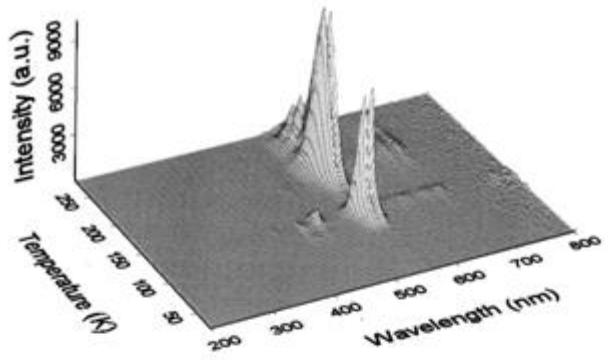

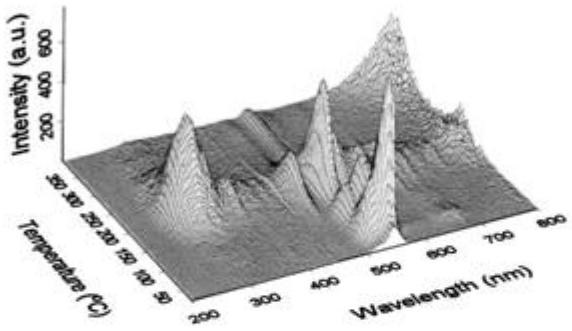

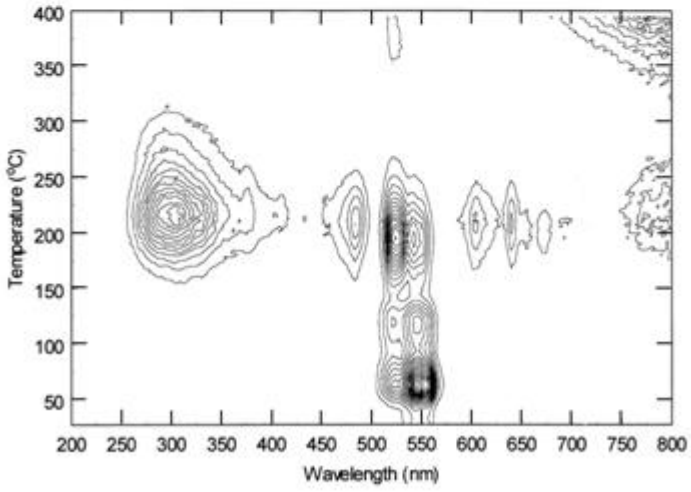

Fig. 9.